Published in final edited form as:

J Immunol. 2018 September 01; 201(5): 1536–1548. doi:10.4049/jimmunol.1701240.

2B4 Mediates Inhibition of CD8+ T Cell Responses via Attenuation of Glycolysis and Cell Division

Sonia J. Laurie[*], **Danya Liu**[*], **Maylene E. Wagener**[*], **Phoebe E. Stark**[*], **Cox Terhorst**[†], and **Mandy L. Ford**[*]

[*]Emory Transplant Center, Atlanta, GA 30322

[†]Beth Israel Deaconess Medical Center, Boston, MA 02215

Abstract

We recently showed that 2B4 expression on memory T cells in human renal transplant recipients was associated with reduced rates of rejection. To investigate whether 2B4 functionally underlies graft acceptance during transplantation, we established an experimental model wherein 2B4 was retrogenically expressed on donor-reactive murine $CD8^+$ T cells (2B4rg), which were then transferred into naïve recipients prior to skin transplantation. We found that constitutive 2B4 expression resulted in significantly reduced accumulation of donor-reactive $CD8^+$ T cells following transplantation, and significantly prolonged graft survival following transplantation. This marked reduction in alloreactivity was due to reduced proliferation of $CD8^+$ $Thy1.1^+$ 2B4rg cells as compared to control cells, underpinned by extracellular flux analyses demonstrating that 2B4 deficient (2B4KO) $CD8^+$ cells activated in vitro exhibited increased glycolytic capacity and upregulation of gene expression profiles consistent with enhanced glycolytic machinery as compared to WT controls. Furthermore, 2B4KO $CD8^+$ T cells primed in vivo exhibited significantly enhanced ex vivo uptake of a fluorescent glucose analog. Finally, the proliferative advantage associated with 2B4 deficiency was only observed in the setting of glucose sufficiency; in glucose-poor conditions 2B4KO $CD8^+$ T cells lost their proliferative advantage. Together, these data indicate that 2B4 signals function to alter T cell glucose metabolism, thereby limiting the proliferation and accumulation of $CD8^+$ T cells. Targeting 2B4 may therefore represent a novel therapeutic strategy to attenuate unwanted $CD8^+$ T cell responses.

INTRODUCTION

A fine balance of costimulatory and coinhibitory signals regulates the activation, differentiation, and proliferation of T cells following encounter with cognate allogeneic peptide:major histocompatibility complexes (pMHC). As such, manipulation of these cosignaling molecules may effectively inhibit unwanted T cell responses during autoimmunity and transplantation. 2B4 (SLAMf4, CD244) is an immunoglobulin (Ig)

Corresponding Author: Mandy L. Ford, Phone number: 404-727-3660, Fax number: 404-727-2900, mandy.ford@emory.edu, Emory Transplant Center, 101 Woodruff Circle, Suite 5105, Atlanta, GA 30322.

AUTHOR CONTRIBUTIONS

SJL and MLF conceived the study and wrote the manuscript. CT provided animals. SJL, DL, and MEW performed the research, and SJL analyzed the data.

superfamily member expressed on natural killer (NK) cells and induced on some $CD8^+$ T cells (1–3). 2B4 contains an immunoreceptor tyrosine-based switch motif (ITSM) and is known to associate with the signaling lymphocytic activation molecule (SLAM)-associated protein (SAP), an intracellular adaptor protein, and bind CD48, a surface Ig molecule widely expressed on hematopoietic cells (4–10). Binding of CD48 to 2B4 can provide costimulatory signals to neighboring T cells via direct cell-to-cell contact (11–13). SAP mediates its function in NK cells via a dual mechanism of action: it augments cell activation by recruiting the kinase Fyn, while simultaneously preventing inhibitory signals by uncoupling SLAM receptors from inhibitory phosphatases (14–17).

Previous studies have shown that 2B4 can be expressed on $CD8^+$ T cells with activated and memory-like phenotypes and the majority of studies suggest that it functions in a coinhibitory capacity to regulate responses on these cells. In particular, 2B4-deficient mice develop a spontaneous lupus-like disease dependent on aberrant T cell activation (18). Further, in mouse models of chronic infection, 2B4 has been shown to limit the expansion and functionality of secondary effector T cells (18, 19). More recently, we found that human transplant recipients that went on to experience stable graft function for at least one year post-transplant exhibited increased frequencies of $2B4^+$ $CD28^{null}$ effector memory T cells (20) at baseline as compared to patients that experienced acute rejection following transplantation (21). These associative data implied that expression of 2B4 on T cells might dampen alloreactive immune responses; however, this hypothesis has not been formally tested, and potential mechanisms underlying it are unknown.

Studies over the last five years have described the impact of changes in cellular metabolism during T cell activation on the programmed differentiation of effector and memory T cell populations (22, 23). Broadly, resting T cells utilize oxidative phosphorylation as their primary source of energy, while effector cells undergoing rapid proliferation switch to aerobic glycolysis in order to meet the energetic needs of an exponentially expanding T cell clonal population (24). Specifically, while oxidative metabolism transitions glucose-derived pyruvate to the mitochondria for oxidation all the way down to carbon dioxide, glycolysis instead generates several key intermediates that the dividing cell can use for biosynthesis (25). Moreover, during aerobic glycolysis, some glucose is funneled through the mitochondria and a portion of the tricarboxylic acid (TCA) cycle in order to generate citrate for the synthesis of lipids necessary for construction of daughter cell membranes. These critical changes are initiated via integration of signals generated by the ligation of the TCR and costimulatory molecules on the T cell surface (26). Both TCR and costimulatory receptors trigger the activation of key signaling pathways that alter gene expression, including c-Myc and the nuclear hormone receptors ERRα, β, and γ and NR3B1, 2, and 3 (26). In addition, CD28 signaling functions to activate the PI3K/Akt/mTOR pathway. Both Akt and mTORC1 activation drive the cell toward aerobic glycolysis and promote the growth and function of effector T cells (27). Importantly, ligation of T cell coinhibitory receptors can also impact T cell metabolism. In particular, ligation of PD-1 was shown to result in a shift from a glycolysis-dependent program to one in which T cells rely more heavily on fatty acid oxidation and lipolysis (28). Additionally, a recent report describes that in samples derived from human patients with gastric cancers, coinhibitory TIGIT signaling on $CD8^+$ T cells inhibits glucose metabolism (29). However, the impact of 2B4 coinhibition

on T cell metabolism and programmed differentiation has been less well studied. Here, we used a retrogenic approach to express 2B4 on antigen-specific $CD8^+$ T cells, in order to understand the effects of 2B4 signaling on $CD8^+$ T cell programmed differentiation and cellular metabolism.

MATERIALS AND METHODS

Mice

C57BL/6 (H-2b) mice were obtained from the National Cancer Institute (Frederick, MD). OT-I (30) and OT-II (31) transgenic mice were purchased from Taconic Farms (Germantown, NY) and bred to $Thy1.1^+$ background at Emory University. mOVA mice (C57BL/6 background, H-2b) (32) were a generous gift from Dr. Marc Jenkins (University of Minnesota, Minneapolis, MN). This study was carried out in strict accordance with the recommendations in the Guide for the Care and Use of Laboratory Animals. The protocol was approved by the Institutional Animal Care and Use Committee of Emory University (protocol number: DAR-2002050-092815GN). All surgery was performed under general anesthesia with maximum efforts made to minimize suffering. All animals were housed in specific pathogen-free animal facilities at Emory University.

Donor-Reactive T Cell Adoptive Transfers

In order to approximate the precursor frequency of donor-reactive cells in a fully MHC mismatched model of transplantation, we utilized our previously described system in which we adoptively transfer a higher frequency of OVA-specific TCR transgenic cells into naïve hosts prior to transplantation. For adoptive transfer of donor-reactive T cells, spleen and mesenteric lymph nodes (mLN) isolated from $Thy1.1^+$ OT-I and $Thy1.1^+$ OT-II mice were processed and stained with monoclonal antibodies for CD8 (Invitrogen), CD4, Thy1.1, and Vα2 (all from BD Pharmingen) for flow cytometric analysis. Cells were resuspended in 1× phosphate buffered saline (PBS) and 10^6 of each $Thy1.1^+$ OT-I and OT-II were injected i.v. 48 hours prior to skin transplantation. Where indicated, OT-I T cells were isolated and labeled with 5 μM CellTrace Violet dye (Life Technologies, Invitrogen) prior to adoptive transfer. Proliferation was measured following sacrifice ten days post-transplantation via flow cytometry on a BD LSR II (BD Biosciences) and data were analyzed with FlowJo (TreeStar) and Prism (GraphPad). Numbers of precursor cells recruited into the anti-donor immune responses were calculated by first multiplying the absolute number of $Thy1.1^+$ $CD8^+$ T cells by the frequency of cells within a given round of division. We then divided the number of cells in each division by 2^n, where n is the number of divisions and the total number of precursors that gave rise to the cells in each division were summed.

Skin Transplantation

Full thickness tail and ear skins were transplanted onto the dorsal thorax of recipient mice and secured with adhesive bandages as previously described (33). Where indicated in Figure 1, recipients were treated with CTLA-4 Ig (abatacept, Bristol-Myers Squibb) (500 μg i.p. on days 0, 2, 4, and 6). In all cases, grafts with less than 10% viable tissue remaining were scored as rejected.

2B4 Plasmid Construction and Transfection

The murine 2B4 gene was derived from mouse cDNA (OriGene: MC209044-113649) and produced by PCR using the primers: (Forward: GCGAATTCGCACCATGTTGGGG CAAGCTGTCCTGTTCACAA, Reverse: CGCTCGAGCTAGGAGTAGACATCAAAGTT CTC). The resulting PCR fragment was cloned into the pMY-IRES-GFP retroviral vector (Cell Biolabs, RV-021) using EcoRI and XhoI cut sites. The Platinum-E retroviral packaging cell line (Cell Biolabs, RV-101. Ecotropic for rat and mouse cells) was used to produce the 2B4-containing retrovirus. The cells were maintained in Dulbecco's modified Eagle's medium (DMEM) supplemented with 10% heat-inactivated fetal calf serum (FCS), 1 μg/ml puromycin, 10 μg/ml blasticidine, 100 U/mL penicillin, and 100 μg/mL streptomycin at 37°C in a 5% CO_2, humidified atmosphere. The packaging cells were incubated in 10-cm plates at 4.5×10^6/plate overnight at 37°C. Transfections were performed with the reagent Lipofectamine LTX (Invitrogen, 15338-100). Cells were transiently transfected with 10 μg DNA (2B4 plasmid DNA or empty-vector control). After 48 hours incubation the culture supernatant was harvested and virus was concentrated per manufacturer's instructions (Cell Biolabs, RV-201).

Retroviral transduction and generation of 2B4rg OT-I T cells

Two days before transduction, bone marrow (BM) cells (BMC) were harvested from 8 to 12 week old OT-I transgenic mice and cultured at 1.5×10^7 cells per 10 cm plate in 15 ml DMEM supplemented with 15% heat-inactivated fetal calf serum (FCS), 100 U/mL penicillin, and 100 μg/mL streptomycin, 10mM HEPES, 20 ng/ml murine interleukin-3 (IL-3), 50 ng/ml human IL-6 and 50 ng/ml murine stem cell factor (SCF) (R&D Systems). Concentrated virus was transduced into the pre-cultured BMCs. After 48 hours incubation bone marrow cells were collected and washed. 4×10^6 bone marrow cells in PBS were injected into sub-lethally irradiated (800 rads) wild type (WT) B6 recipients. Splenocytes from these BM chimeras were harvested 6-8 weeks post-transfer and were enriched by negative selection using a $CD8\alpha^+$ T cell Isolation Kit II (Miltenyi Biotec,). Purity of $CD8\alpha^+$ T cells was between 60 and 85%. Cells were then stained with anti-CD8 (Invitrogen), anti-Thy1.1 (BD Biosciences), and anti-2B4 (BD Biosciences) and GFP^+ $CD8^+$ $Thy1.1^+$ $2B4^+$ cells were purified by FACS sorting on a BD FACS Aria (BD Biosciences). Post-sort 2B4-OT-I T cell populations were over 94% pure. Cells were resuspended in PBS with 10^6 wild-type $CD4^+$ $Thy1.1^+$ OT-II T cells and injected i.v. 48 hours prior to skin transplantation. Where indicated, retrogenic cells were prepared from the spleen and transferred i.v. without sorting along with wild-type $CD4^+$ $Thy1.1^+$ OT-II T cells 48 hours prior to skin transplantation. Upon sacrifice of the recipients ten days following transplantation, these cells were analyzed separately form bulk splenocytes via flow cytometric gating.

Flow Cytometry and Intracellular Cytokine Staining

Cells isolated from spleens and graft-draining axillary and brachial lymph nodes (dLN) were stained with anti-CD4 (BD Biosciences), anti-CD8 (Invitrogen) and anti-Thy1.1 (BD Biosciences). For phenotypic analysis cells were also surface-stained with anti-PD-1 (BioLegend), anti-2B4 (BD Biosciences or eBioSciences), anti-Thy1.1 (BD Biosciences), anti-LAG-3 (BioLegend), anti-CD127 (BioLegend), anti-KLRG-1 (eBioSciences), anti-

CD44 (BioLegend or BD Biosciences), and anti-CD48 (BioLegend). Absolute numbers of lymphocytes from the spleen and draining lymph nodes were calculated using a Cellometer Auto T4 Cell Viability Counter (Nexcelom) according to the manufacturer's instructions. Samples were analyzed on an LSRII flow cytometer (BD Biosciences). Data was analyzed using FlowJo 9 software (Treestar, San Carlos, CA) and Prism 6 software (GraphPad Software Inc.). For intracellular cytokine staining, lymphocytes were restimulated *ex vivo* with 1 μg/mL phorbol 12-myristate 13-acetate (PMA) (Sigma Life Sciences) and 1 μg/mL ionomycin (Sigma Life Sciences) where indicated, in the presence of 1 μg/mL Brefeldin A (BD Biosciences) for 4 hours. The Fix/Perm intracellular staining kit (BD Pharmingen) was used to detect IL-2 (BD Biosciences), TNF (BioLegend), and IFN-γ (BD Biosciences), according to manufacturer's instructions.

RT-PCR Analysis

Splenocytes were isolated and prepared as a single-cell suspension. 3×10^6 WT and 2B4KO OT-I T cells, respectively, were resuspended in 1.5 mL of complete media (RPMI-1640 supplemented with 10% FCS, 2 mM L-glutamine), 100 U/mL penicillin, 100 μg/mL streptomycin, 10 mM HEPES, and 0.5 mM 2-mercaptoethanol) in a 24-well flat-bottomed plate at 37°C in a 5% CO_2, humidified atmosphere. Cells were then stimulated with SIINFEKL N4 peptide at 1 nM for 4 days. After 4 days cells were collected and live cells were isolated via Ficoll gradient separation. 1×10^6 live cells were plated with 5×10^6 naïve splenocytes stimulator cells isolated from WT C57BL/6 donors and restimulated with 1 nM SIINFEKL peptide for four additional days in a final volume of 1.5 mL in a 24-well flat-bottomed plate at 37°C in a 5% CO_2, humidified atmosphere. Following restimulation, cells were harvested and incubated with Pacific Orange anti-CD8 (Invitrogen), PerCP anti-Thy1.1 (BD Biosciences), and PE-Cy7 anti-CD244 (eBioSciences) for 30 minutes at 4°C. Following staining, cells were washed with sterile 1× PBS and resuspended in ~1 mL of sorting buffer (sterile 1× PBS with 2% serum and 1 mM EDTA). Cells were sorted on FACSAriaII (BD Biosciences) and 2B4KO and $2B4^+$ OT-I T cells were isolated to at least 90% purity. FACS-purified cells were then resuspended in RLT buffer with β-ME (Qiagen, 350 μl for $>5\times10^6$ cells, 600 μl for $<5\times10^6$ cells) and flash frozen on dry ice for 10 minutes prior to storage at -80°C. RNA was isolated from previously frozen cells using the RNEasy Mini Kit (Qiagen, Germantown, MD) and quantified using a Nanodrop Microvolume Spectrophotometer (Thermofisher, Waltham, MA). RNA was converted to cDNA using the RT^2 First Strand Kit (Qiagen), and RT-PCR was performed using the Qiagen Glucose Metabolism RT^2 Profiler PCR Array with the RT^2 SYBR Green qPCR Mastermix (Qiagen) on a BioRad CFX384 Touch Real-Time PCR Detection System. Data was analyzed online via the Qiagen GeneGlobe Data Analysis Center.

Seahorse XF Glycolysis Stress Test

Splenocytes were isolated and stimulated for four days as described above. Following Ficoll separation, 2×10^5 OT-I live cells were then plated in buffer-free, glucose-free XF assay media (Agilent Technologies) supplemented with 2 mM L-glutamine, pH 7.4+/0.1. Extracellular acidification rate (ECAR) was measured and recorded at basal conditions as well as at indicated time points following the addition of glucose (final concentration 10 mM/well), oligomycin (final concentration 1 μM/well), and 2-deoxyglucose (final

concentration 50 mM/well), using a Seahorse XFe96 Analyzer (Agilent Technologies). Basal ECAR readings were generated from the average of five measurements prior to the addition of oligomycin, while maximal ECAR was calculated from the average of three measurements following the addition oligomycin.

In vitro Glucose-limiting Stimulation Assays

Splenocytes were isolated and prepared as a single-cell suspension. 3×10^6 WT and 2B4KO OT-I T cells, respectively, were resuspended in 1.5 mL of complete media (glucose-free RPMI-1640 supplemented with 10% FCS, 2 mM L-glutamine), 100 U/mL penicillin, 100 μg/mL streptomycin, 10 mM HEPES, and 0.5 mM 2-mercaptoethanol) in a 24-well flat-bottomed plate at 37°C in a 5% CO_2, humidified atmosphere. A D-glucose solution of 200g/L (Gibco by Life Technologies) was titered into the glucose-free complete media and diluted on a half-log scale. Cells were then stimulated with SIINFEKL N4 peptide at 1 nM for 5 days. After 5 days in culture cells were harvested and stained with anti-CD8 (BD Horizon), anti-Thy1.1 (BD Biosciences or BioLegend), anti-CD244 (eBioSciences), anti-Va2 (BD), anti-CD127 (BioLegend), anti-CD62L (BD), anti-KLRG-1, anti-Vb5 (BD), anti-CD44 (BD), 7AAD (BD) and AnnexinV (BioLegend), anti-IL-2 (BD), anti-IFN-g (BD) as described by the manufacturer. As described above, samples were analyzed on an LSRII flow cytometer (BD Biosciences) and data was analyzed using FlowJo 9 software (Treestar, San Carlos, CA) and Prism 6 software (GraphPad Software Inc.).

2-NBDG Uptake Assay

To assess the ability of 2B4-deficient OT-I T cells to take up glucose, 10^4 WT and 2B4KO OT-I T cells were transferred into naïve C57BL/6 hosts and infected them with 10^4 colony forming units (CFU) of OVA-expressing *Listeria monocytogenes* (LM-OVA) two days. 14 days after infection, the animals were sacrificed and spleens were harvested. The cells were isolated and resuspended in a single cell solution in PBS. 2×10^6 splenocytes were stained with anti-CD4 (BD Biosciences), anti-CD8 (Invitrogen) and anti-Thy1.1 (BD Biosciences), anti-CD44 (eBioSciences), anti-CD44 (BD Biosciences) for 30 minutes at 4°C. Cells were washed twice in 250 μl of PBS and then resuspended in 200 μl of 50 μM 2-NBDG (Thermofisher) and incubated at 37°C for 30 minutes. Cells were washed with PBS and then analyzed on an LSRII flow cytometer (BD Biosciences). Data was analyzed using FlowJo 9 software (Treestar) and Prism 6 software (GraphPad Software Inc.).

Statistical Analysis

T cell responses were analyzed using unpaired, non-parametric Mann-Whitney t-tests. Results were considered significant if $p < 0.05$. Survival curves were analyzed by log-rank test and plotted on Kaplan-Meier curves. All analyses were done using Prism software (GraphPad Software Inc.).

RESULTS

Ectopic expression of 2B4 on donor-reactive CD8$^+$ T cells results in prolongation of allograft survival

Given the observation that increased 2B4 expression was associated with reduced incidence of rejection in renal transplant recipients treated with belatacept (21), we investigated the causal role of 2B4 expression in attenuating donor-reactive CD8$^+$ T cell responses following transplantation. To test this we utilized a retrogenic approach to generate donor-reactive CD8$^+$ T cells that constitutively express 2B4 (2B4rg). Though primary effector cells do not express 2B4 at baseline (Figure 1E), we have previously identified an association between 2B4 expression on T cells and improved graft survival in both murine models and human transplant recipients (21, 34). Thus, we aimed to create a system in which we could isolate and interrogate this effect, and in which we would be able to determine if upregulation of 2B4 can functionally impact alloreactive T cell responses. To this end, we utilized retrovirally-transduced bone marrow derived from OT-I mice with a 2B4-bearing construct or an empty control vector. Transduced cells express GFP under the control of the IRES promoter, allowing us to identify, isolate, and track these cells in both in vivo and in vitro assays. Briefly, CD45.2$^+$ Thy1.1$^+$ OT-I bone marrow was transduced with a construct that expresses 2B4 under a constitutively active viral promoter and contained an IRES-GFP to facilitate tracking the cells. At day 2 post transduction, ~5–10% of Thy1.1$^+$ OT-I BM cells expressed GFP alone (for pMY control vector-transduced cells) or both GFP and 2B4 (for 2B4 vector-transduced cells) (Figure 1A). BM cells were then adoptively transferred into irradiated CD45.1$^+$ Thy1.2$^+$ animals. At 8–10 weeks post-in vivo transfer, GFP labeled Thy1.1$^+$ OT-I T cells were detectable in recipients of 2B4 vector-transduced and pMY control vector-transduced BM cells at similar frequencies (Figure 1B), suggesting that 2B4 expressing OT-I T cells mature normally in these animals. GFP$^+$ CD8$^+$ Thy1.1$^+$ (for pMY) or GFP$^+$ 2B4$^+$ CD3$^+$ Thy1.1$^+$ (for 2B4rg) OT-I T cells were isolated from the spleen and mesenteric lymph nodes of pMY or 2B4rg chimeric animals and then MACS and FACS sorted to >86% purity (Figure 1C).

To determine the impact of constitutive 2B4 expression on graft-specific alloimmune responses, naïve B6 animals were adoptively transferred with 10^6 congenically labeled 2B4rg Thy1.1$^+$ OT-I T cells (or pMY Thy1.1$^+$ OT-I controls) along with 10^6 Thy1.1$^+$ CD4$^+$ WT OT-II T cells and then challenged with an OVA-expressing skin graft (Figure 1D). Animals were sacrificed at day 10 post-transplant, the magnitude of the CD8$^+$ Thy1.1$^+$ response was assessed. Importantly, expression of 2B4 was maintained in the 2B4rg OT-I T cells during the *in vivo* response (Figure 1E). To determine the impact of donor-reactive CD8$^+$ T cell 2B4 expression on graft survival, recipients of either 2B4rg or control OT-I T cells were monitored for graft survival. Under these conditions, we saw no difference in graft survival (not shown). Likewise, there was also no difference in graft survival when OT-I T cells were WT vs. 2B4 KO (data not shown). To test whether or not expression of 2B4 can prolong graft survival in the context of minimal immunotherapy, we adoptively transferred 2B4rg OT-I T cells into animals that received a low dose of CTLA4Ig in the first week following transplantation in order to extend graft survival enough to allow us to see any potential differences in survival between animals that received the WT vs. 2B4KO cells.

Results indicated a significant prolongation in survival in recipients of 2B4rg donor-reactive $CD8^+$ T cells as compared to recipients of control donor-reactive $CD8^+$ T cells (MST 31.5 vs. 23, p=0.01) (Figure 1F).

Ectopic expression of 2B4 resulted in reduced accumulation of antigen-specific $CD8^+$ T cells

In order to investigate the mechanisms underlying the observed prolongation in graft survival in CTLA-4Ig-treated graft recipients possessing 2B4rg donor-reactive $CD8^+$ T cells, spleens and draining LN were harvested on day 10 post-transplantation and the magnitude and functionality of the $Thy1.1^+$ $CD8^+$ T cell response was assessed. Results revealed detectable populations of $CD44^{hi}$ $Thy1.1^+$ $CD8^+$ T cells in the spleens and lymph nodes (data not shown) of mice that received either pMY or 2B4rg OT-I T cells, respectively (Figure 2A). Strikingly, constitutive expression of 2B4 resulted in significantly decreased accumulation of donor-specific $CD44^{hi}$ $Thy1.1^+$ $CD8^+$ T cells in the spleen following transplantation in the absence of any further immune modulation, both in terms of frequency and absolute number (Figure 2B). In contrast, retrogenic 2B4 expression did not significantly impair production of IFN-γ on a per cell basis following *ex vivo* restimulation (Figure 2C and 2D), though fewer total cytokine-secreting OT-I T cells could be detected in the spleen 10 days following transplantation (Figure 2E). Taken together, these results indicate that expression of 2B4 on $CD44^{hi}$ $Thy1.1^+$ $CD8^+$ T cells results in the attenuation of graft-specific T cell responses in the spleen 10 days following transplantation.

Failure of 2B4 retrogenic cells to accumulate in the spleen is not due to differences in expression of the 2B4 ligand CD48, T cell activation or exhaustion markers, or T cell death

We next investigated whether or not the reduced accumulation of $Thy1.1^+$ $CD8^+$ T cells in the spleens of 2B4rg recipients was due to differences in the activation, differentiation, or exhaustion status of these cells. In experiments similar to those described above, naïve B6 animals were adoptively transferred with 10^6 congenically labeled 2B4rg $Thy1.1^+$ OT-I T cells or pMY controls, along with 10^6 $Thy1.1^+$ $CD4^+$ WT OT-II T cells, challenged with an OVA-expressing skin graft, and sacrificed at day 10 post transplant at which time splenic T cells were stained for markers of activation, differentiation, and exhaustion and analyzed by flow cytometry. Analysis of cell surface phenotypes indicates there was no difference in the activation status of the 2B4rg $Thy1.1^+$ OT-I T cells when compared to the pMY $Thy1.1^+$ OT-I controls as measured by CD44 expression (Figure 3A). There was also no detectible difference in the presence of short-lived vs. memory precursor effector cells as distinguished by CD127 and KLRG-1 staining (Figures 3A, 3B and 3C). Additionally, no differences were found in the expression of PD-1 and lymphocytes activation gene 3 (LAG-3) exhaustion markers on 2B4rg vs. pMY $Thy1.1^+$ OT-I T cells (Figures 3A, 3D and 3E). Finally, the expression of the 2B4 ligand CD48 did not differ between the 2B4rg $Thy1.1^+$ OT-I or pMY $Thy1.1^+$ OT-I control cells (Figures 3A and 3F). Overall, these data suggest that the failure of 2B4rg $Thy1.1^+$ OT-I cells to accumulate in the spleen after transplantation was not due to differences in their expression of the 2B4 ligand or T cell activation or exhaustion markers. We therefore next sought to determine whether the paucity of 2B4rg cells observed in the spleen 10 days after transplantation was due to increased cell death. As depicted in Figure 3G, no increase in cell death as measured by Annexin V^+ 7-AAD^+ double-positivity was

observed in the 2B4rg Thy1.1$^+$ OT-I T cells as compared to pMY controls. Instead, 2B4rg OT-I T cells actually exhibited reduced frequencies of Annexin V$^+$ 7-AAD$^+$ cells (Figure 3H). These data therefore demonstrate that the observed reduced accumulation of 2B4rg graft-specific CD8$^+$ T cells was not due to increased cell death within the 2B4rg compartment.

2B4 rg OT-I T cell population exhibits less division compared to pMY control OT-I due to reduced recruitment into the anti-donor immune response

Because the above experiments failed to explain impaired accumulation of 2B4-expressing CD8$^+$ T cells following transplantation, we next asked if the reduced accumulation of 2B4rg graft-specific OT-I T cells following transplantation was the result of differences in the amount of cell division following activation. To test this, GFP$^+$ CD8$^+$ Thy1.1$^+$ OT-I T cells were isolated from spleen and mLN of 2B4rg chimeric animals and stained with CellTrace Violet prior to being adoptively transferred (10^6/recipient) into naïve B6 hosts that received 10^6 WT CD4$^+$ Thy1.1$^+$ OT-II T cells and were grafted with an OVA-expressing skin graft. As previously described, animals were sacrificed on day 10 post-transplant 2B4rg chimeric cells were isolated from the spleen analyzed by flow cytometry. Our analyses revealed striking differences between the frequency and number of GFP$^+$ CD8$^+$ Thy1.1$^+$ OT-I T cells dividing in the 2B4rg and non-retrogenic compartments (Figures 4A, 4B and data not shown). The frequency of OT-I cells that underwent 4 or more rounds of division was significantly lower in the 2B4rg OT-I populations as compared to the GFP single-positive controls (Figures 4C and 4D). Furthermore, we observed a statistically significant increase in the number of 2B4rg OT-I that remained undivided 10 days following transplantation as compared to pMY OT-I controls (Figure 4E). Additional analyses of cell division calculating the number of precursors that were recruited into the response (based on the number of cells present in each CTV peak at day 10 as described in materials and methods) revealed that fewer 2B4rg OT-I precursors were recruited into the response as compared to pMY OT-I precursors (Figure 4F). Taken together, these findings demonstrate that expression of 2B4 impairs expansion of the anti-donor CD8$^+$ effector population by preventing cells from entering the cell cycle.

2B4 expression limits glycolytic capacity of CD8$^+$ T cells

To determine the mechanism by which constitutive expression of 2B4 impairs proliferation of anti-donor CD8$^+$ T cells, we next assessed T cell metabolism. It is known that T cells undergo metabolic reprogramming as they differentiate into effectors, and that glycolysis is the primary method by which these cells derive the energy needed to proliferate during this process (35, 36). As bioenergetic needs of T cells are significantly augmented during this critical time, it is possible to detect a notable increase in the uptake and utilization of glucose soon after activation (37). To address whether or not glycolysis was altered in the absence of 2B4, we utilized a model in which we stimulated WT and 2B4-deficient (2B4KO) OT-I T cells in vitro and then probed their metabolic capacity. To test the hypothesis that 2B4 signaling limits CD8$^+$ T cell proliferation by inhibiting glycolysis, we established a model in which WT and 2B4KO OT-I T cells were stimulated in culture for seven days with their cognate peptide SIINFEKL, purified via Ficoll gradient centrifugation, and then restimulated for four more days in vitro. After restimulation, 2B4$^+$ cells were purified to >90% purity

from WT OT-I T cells by FACS sorting, and 2B4KO OT-I T cells were confirmed to be $2B4^-$ by flow cytometry. Following sorting, we assessed the expression of 84 genes associated with glucose metabolism in $2B4^+$ WT vs. 2B4 KO cells using the Qiagen Glucose Metabolism RT^2 Profiler PCR Array. Of the 84 genes assessed in this array, we noted that 42 were differentially expressed between $2B4^+$ OT-I cells isolated from WT animals and 2B4KO OT-I T cells (Figure 5A). Of those, a number were associated with glycolytic shifts in response to activation, the pentose phosphate pathway, the TCA cycle, and in aerobic glycolysis (Figure 5B).

Based on the differential expression of genes in the glycolytic pathways identified via transcriptional profiling, we next endeavored to assess functional changes in T cell metabolism based on 2B4 expression using the Seahorse XFe96 Analyzer. As demonstrated in Figures 5C, we found that the loss of 2B4 on antigen-specific T cells results in enhanced glycolytic metabolism as measured by an increase in extracellular acidification rate (ECAR) during glucose-induced glycolysis (38). Additionally, we observed that the ability of OT-I T cells to perform glucose-induced glycolysis was greater in the absence of 2B4, and that the total glycolytic capacity of the 2B4KO cells was greater than that of the wild type controls (Figure 5D-E). Next, to determine whether 2B4KO T cells achieved increased glycolytic capacity in part via increasing their uptake of glucose from the extracellular environment, we moved to an in vivo model of T cell stimulation followed by ex vivo incubation with the fluorescent glucose analog 2-NBDG (Figure 5E-G). Because WT graft-elicited $CD8^+$ T cell responses did not exhibit high frequencies of 2B4-expressing cells (Figure 2 and (34)), we moved to a model of bacterial infection. Briefly, 14 days following infection with OVA-expressing *Listeria monocytogenes*, 2×10^6 cells were plated directly ex vivo and incubated with 2-NBDG for 30 minutes, and uptake was determined by assessing fluorescence via flow cytometry. Data indicated that uptake of 2-NBDG was significantly increased in 2B4KO $CD8^+$ T cells as compared to WT $CD8^+$ T cells (Figure 5F–5G).

Proliferative advantage of 2B4 KO T cells is erased under glucose limiting conditions

Our data thus far demonstrated increased proliferation and increased glycolysis in the setting of 2B4 deficiency. In order to identify a causal link between these two observations, we queried whether the proliferative advantage observed in 2B4 KO T cells would persist under glucose-restrictive conditions. To test this, WT and 2B4KO OT-I T cells were labeled with CellTrace Violet prior to stimulation with SIINFEKL N4 peptide at 1 nM in media containing varying concentrations of glucose as described in Materials and Methods and Figure 6A. Our results demonstrate that 2B4KO OT-I T cells restimulated in glucose-replete media exhibited a statistically significant increase in CTV dilution relative to WT control cells (Fig. 6B-C) as expected, demonstrating that 2B4 deficiency confers a proliferative advantage when glucose is abundant, in these experiments at the level of 3 mM or higher. In contrast, when glucose was present only at low levels (1 mM or less) WT and 2B4KO OT-I T cells exhibited similar levels of CTV dilution (Fig. 6B, 6C). To rule out the possibility that measured proliferation of these cells may have been impacted by increased rates of cell death in the cultures with low glucose, we assessed apoptosis by quantifying the frequency of 7AAD and AnnexinV double-positive cells and show that there were no differences between death of WT and 2B4KO cells in any culture condition (Fig. 6D). These data thus

suggest that the observed differential proliferation of 2B4KO T cells is dependent on their ability to undergo increased glycolytic metabolism.

2B4-mediated signals impact CD8$^+$ T cell memory recall potential

To determine whether or not enhanced glycolytic capacity following activation impacts the functionality of 2B4KO T cells, we transferred WT and 2B4KO OT-I T cells into naïve C57BL/6 hosts and then infected them with OVA-expressing *Listeria monocytogenes* (LM-OVA) two days later (Fig. 7A). Ten days later, each animal received an OVA-expressing skin graft (Fig. 7A). Animals were sacrificed five days following transplantation, and spleens as well as axillary and brachial draining lymph nodes were harvested for analysis. In comparison to the wild type controls, graft-specific cells lacking 2B4 express less KLRG-1 (Figure 7B, 6C), which has been suggested to be associated with a senescent-like program (40). Additionally, the 2B4KO cells express higher levels of CXCR3 and CD69 (Figure 7B, 6C), consistent with a model in which the loss of 2B4 results in a more activated phenotype. CD44 expression was not different between the two cell types (Fig. 7B-C). Strikingly, we found in addition to their activated phenotype, graft-specific 2B4 KO CD8$^+$ Thy1.1$^+$ secondary effectors contained a higher frequency of IFN-γ^+ IL-2$^+$ double producers upon rechallenge with a skin graft as compared to WT CD8$^+$ Thy1.1$^+$ cells (Fig. 7D, 6E). These data support the conclusion that loss of 2B4 coinhibitory signaling on CD8$^+$ donor-reactive T cells results in enhanced metabolism and altered memory T cell differentiation that leads to more robust secondary recall responses following rechallenge.

DISCUSSION

In this study, we showed that constitutive expression of 2B4 prolongs allograft survival and limits alloreactivity by attenuating the accumulation of donor-specific CD8$^+$ T cells following transplantation (Figs. 1A, B). Our data reveal increased T cell glycolytic metabolism in the absence of 2B4, demonstrated both functionally using the Seahorse extracellular flux assay as well as by analysis of changes in expression of 84 metabolism-associated genes. Of note, genes upregulated in activated 2B4-deficient CD8$^+$ T cells were associated with glycolytic machinery, the pentose phosphate pathway, the TCA cycle, and aerobic glycolysis. For example, *Eno2* and *Eno3*, encode Enolases 2 and 3, metalloenzymes responsible for the catalysis of the conversion of 2-phosphoglycerate (2-PG) to phosphoenolpyruvate (PEP), the ninth and penultimate step of glycolysis. We also noted an increase in *G6pdx* in cells deficient in 2B4 (Fig 5B). *G6pdx* encodes glucose-6-phosphate dehydrodgenase X-linked, a key enzyme in the pentose phosphate pathway, a mechanism of generating energy that is strongly relied upon by proliferating T cells (43). Additionally, the enhanced presence of transcripts for *Pdk1*, which encodes pyruvate dehydrogenase kinase 1, in the absence of 2B4, suggests that 2B4-mediated signaling may promote aerobic glycolysis by inhibiting the activity of pyruvate dehydrogenases (22). Overall, these findings on the impact of 2B4 on T cell metabolism are consistent with recent studies showing that T cell coinhibitory molecules can impact immunometabolism. For example, signaling via PD-1 on activated T cells was shown to prevent glycolysis (36). Similarly, work from Wherry and colleagues recently showed that PD-1 signaling impacts early glycolytic activity in T cells and represses the transcriptional regulator PCG-1a; forced overexpression of PGC-1a was

able to improve the functionality of exhausted T cells (44). Interestingly, PD-1 signaling also augmented lipolysis and β-oxidation of fatty acids, leading to a marked increase in mitochondrial spare respiratory capacity (SRC) (36). PD-1-mediated reinforcement of FAO may serve to explain long-term preservation of these cells during cancer and persistent viral infection. In support of this, recent work has shown that signaling via PD-1 activates AMP-activated protein kinase (AMPK), which is required for the survival and longevity of T cells in nutrient-compromised microenvironments (45). Together with these published studies on the role of PD-1, our data further highlight the emerging role for coinhibitory molecules in the control of T cell bioenergetics and metabolism.

While our study demonstrates that signaling via 2B4 on antigen-specific $CD8^+$ T cells modulates glycolytic metabolism, further studies are needed to assess the impact of this coinhibitor on alternative mechanisms of energy generation, such as fatty acid oxidation. Our data indicate that *Idh2* and *Idh3a* are increased in the absence of 2B4 (Figure 5B). These genes encode isocitrate dehydrogenases that are critical in the tricarboxylic acid (TCA) cycle, which has been shown to be increased in activated T cells, but not to the same degree as glycolysis (46), more work is warranted to dissect a possible role of oxidative metabolism in contributing to T cell function and fate in the presence or absence of 2B4.

Our data also reveal an impact of 2B4-mediated metabolic alterations on programmed T cell differentiation; specifically, 2B4-deficient OT-I cells exhibited enhanced effector recall potential after rechallenge when compared to the wild-type controls (Fig. 7). Thus, 2B4 deficient cells exhibit increased glycolytic metabolism during primary differentiation but also augmented recall responses. These findings of increased glycolytic function being associated with improved recall responses are seemingly at odds with work from Sukumar and colleagues, which showed that enhanced glycolytic flux promotes a state of terminal differentiation, while inhibiting it promotes the generation of long-lived memory $CD8^+$ T cells (47). More recent work, however, has shown that the division of effector-like and memory-like $CD8^+$ T cells into populations that rely on glycolysis and oxidative phosphorylation of fatty acids, respectively, is not so clear cut. For example, van der Windt et al. showed that memory $CD8^+$ T cells exhibit both increased glycolysis and oxidative phosphorylation as compared to primary effectors (48), and a more recent study demonstrated that elevated oxidative phosphorylation is dispensable for the ability of T cells to form long-lived stable memory following an acute infection (38). In line with these findings, the results that we present here demonstrate that the enhanced glycolytic capacity and 2-NBDG uptake observed in the absence of 2B4 (Fig. 5) is correlated with enhanced memory recall potential following rechallenge (Fig. 7). These findings further are supported by a recent study demonstrating that the differentiation of $CD8^+$ effector memory T cells during persistent viral infection was supported by consistent glycolytic metabolism (38); the mechanisms by which immunometabolism controls memory T cell differentiation remains an area of intense investigation.

It is interesting to note that ectopic 2B4 expression resulted in a trend toward decreased effector cytokine production by antigen-specific primary $CD8^+$ T cells on a per cell basis (Fig. 2C-E), and a statistically significant decrease in the absolute number of IFN-γ-secreting cells per spleen. Likewise, the absence of 2B4 on secondary effectors conversely

enhanced cytokine production following antigenic rechallenge (Fig. 4B and C). We speculate that this attenuation in cytokine effector function by 2B4 signaling is mediated by altered immunometabolism. Indeed, a recent report demonstrated that conversion to glycolysis is required for effective IFN-γ production, and showed that this requirement is due to the binding of the glycolysis enzyme GAPDH to AU-rich elements within the 3' UTR of IFN-γ mRNA (49). Thus, expression of GAPDH induced by aerobic glycolysis controls effector cytokine production. These data support our hypothesis that 2B4-mediated regulation of glycolytic metabolism in T cells affects effector function.

Finally, the results presented in our study suggest that as a regulator of metabolism, 2B4 may be an important therapeutic target in the design of new strategies to control donor-reactive T cells following transplantation. Indeed, recent work demonstrated that the blockade of both glycolysis and glutamine metabolism results in the prevention of allograft rejection in a model of fully MHC-mismatched skin and cardiac transplantation, suggesting that the manipulation of effector cell metabolism is an important mechanism by which alloimmunity can be controlled (35). In this study we present data suggesting that engagement of 2B4 can negatively regulate donor-reactive T cell responses in the context of transplantation. This is of translational importance, as we have recently published that not all alloreactive T cells are targeted by the CD28 costimulation blocker belatacept following transplantation, and that those that express low levels of CD28 express high levels of 2B4 (20, 50, 51). In sum, our study suggests that agonistic ligation of 2B4 may be a novel target for therapeutic manipulation to control unwanted T cell responses in the setting of transplantation and autoimmunity.

Acknowledgments

We thank Dr. Jennifer Robertson for her assistance with flow cytometry, and Mr. Aaron Rae (Emory + Children's Pediatric Research Flow Cytometry Core) and Mr. Robert Karaffa (Emory Flow Cytometry Core) for FACS sorting.

This work was supported by NIH R01 AI104699 (to MLF), T32 AI007610, and F30 AI114250 (to SJL).

References

1. Crawford A, Wherry EJ. The diversity of costimulatory and inhibitory receptor pathways and the regulation of antiviral T cell responses. Curr Opin Immunol. 2009; 21:179–86. [PubMed: 19264470]
2. Mooney JM, Klem J, Wülfing C, Mijares LA, Schwartzberg PL, Bennett M, Schatzle JD. The Murine NK Receptor 2B4 (CD244) Exhibits Inhibitory Function Independent of Signaling Lymphocytic Activation Molecule-Associated Protein Expression. The Journal of Immunology. 2004; 173:3953–61. [PubMed: 15356144]
3. Waggoner SN, Kumar V. Evolving role of 2B4/CD244 in T and NK cell responses during virus infection. Front Immunol. 2012; 3:377. [PubMed: 23248626]
4. McNerney ME, Guzior D, Kumar V. 2B4 (CD244)-CD48 interactions provide a novel MHC class I-independent system for NK-cell self-tolerance in mice. Blood. 2005; 106:1337–40. [PubMed: 15870174]
5. Latchman Y, McKay PF, Reiser H. Identification of the 2B4 molecule as a counter-receptor for CD48. J Immunol. 1998; 161:5809–12. [PubMed: 9834056]
6. Kim EO, Kim TJ, Kim N, Kim ST, Kumar V, Lee KM. Homotypic cell to cell cross-talk among human natural killer cells reveals differential and overlapping roles of 2B4 and CD2. J Biol Chem. 2010; 285:41755–64. [PubMed: 20813844]

7. Elishmereni M, Levi-Schaffer F. CD48: A co-stimulatory receptor of immunity. Int J Biochem Cell Biol. 2011; 43:25–8. [PubMed: 20833258]
8. Zamora J, Korb S, Bentt L, Allston C, Jonsson J, Currier C, Light JA. Eosinophiluria as an indicator of kidney-pancreas transplant rejection. Transplant Proc. 1993; 25:948–50. [PubMed: 8442276]
9. Chen L, Flies DB. Molecular mechanisms of T cell co-stimulation and co-inhibition. Nat Rev Immunol. 2013; 13:227–42. [PubMed: 23470321]
10. Chen R, Relouzat F, Roncagalli R, Aoukaty A, Tan R, Latour S, Veillette A. Molecular dissection of 2B4 signaling: implications for signal transduction by SLAM-related receptors. Mol Cell Biol. 2004; 24:5144–56. [PubMed: 15169881]
11. Kambayashi T, Assarsson E, Chambers BJ, Ljunggren HG. Cutting edge: Regulation of CD8(+) T cell proliferation by 2B4/CD48 interactions. J Immunol. 2001; 167:6706–10. [PubMed: 11739483]
12. Lee KM, Bhawan S, Majima T, Wei H, Nishimura MI, Yagita H, Kumar V. Cutting edge: the NK cell receptor 2B4 augments antigen-specific T cell cytotoxicity through CD48 ligation on neighboring T cells. J Immunol. 2003; 170:4881–5. [PubMed: 12734329]
13. Assarsson E, Kambayashi T, Persson CM, Ljunggren HG, Chambers BJ. 2B4 co-stimulation: NK cells and their control of adaptive immune responses. Mol Immunol. 2005; 42:419–23. [PubMed: 15607793]
14. Le Borgne M, Shaw AS. SAP signaling: a dual mechanism of action. Immunity. 2012; 36:899–901. [PubMed: 22749348]
15. Dong Z, Davidson D, Perez-Quintero LA, Kurosaki T, Swat W, Veillette A. The adaptor SAP controls NK cell activation by regulating the enzymes Vav-1 and SHIP-1 and by enhancing conjugates with target cells. Immunity. 2012; 36:974–85. [PubMed: 22683124]
16. Eissmann P, Beauchamp L, Wooters J, Tilton JC, Long EO, Watzl C. Molecular basis for positive and negative signaling by the natural killer cell receptor 2B4 (CD244). Blood. 2005; 105:4722–9. [PubMed: 15713798]
17. Detre C, Keszei M, Romero X, Tsokos GC, Terhorst C. SLAM family receptors and the SLAM-associated protein (SAP) modulate T cell functions. Semin Immunopathol. 2010; 32:157–71. [PubMed: 20146065]
18. Brown DR, Calpe S, Keszei M, Wang N, McArdel S, Terhorst C, Sharpe AH. Cutting edge: an NK cell-independent role for Slamf4 in controlling humoral autoimmunity. J Immunol. 2011; 187:21–5. [PubMed: 21622868]
19. West EE, Youngblood B, Tan WG, Jin HT, Araki K, Alexe G, Konieczny BT, Calpe S, Freeman GJ, Terhorst C, Haining WN, Ahmed R. Tight regulation of memory CD8(+) T cells limits their effectiveness during sustained high viral load. Immunity. 2011; 35:285–98. [PubMed: 21856186]
20. Espinosa J, Herr F, Tharp G, Bosinger S, Song M, Farris AB 3rd, George R, Cheeseman J, Stempora L, Townsend R, Durrbach A, Kirk AD. CD57(+) CD4 T Cells Underlie Belatacept-Resistant Allograft Rejection. Am J Transplant. 2016; 16:1102–12. [PubMed: 26603381]
21. Cortes-Cerisuelo M, Laurie SJ, Mathews DV, Winterberg PD, Larsen CP, Adams AB, Ford ML. Increased Pretransplant Frequency of CD28+ CD4+ TEM Predicts Belatacept-Resistant Rejection in Human Renal Transplant Recipients. Am J Transplant. 2017
22. Buck MD, O'Sullivan D, Pearce EL. T cell metabolism drives immunity. The Journal of Experimental Medicine. 2015; 212:1345–60. [PubMed: 26261266]
23. Pearce EL, Poffenberger MC, Chang CH, Jones RG. Fueling immunity: insights into metabolism and lymphocyte function. Science. 2013; 342:1242454. [PubMed: 24115444]
24. Almeida L, Lochner M, Berod L, Sparwasser T. Metabolic pathways in T cell activation and lineage differentiation. Seminars in Immunology. 2016; 28:514–24. [PubMed: 27825556]
25. MacIver NJ, Rathmell JC. Editorial overview: Metabolism of T cells: integrating nutrients, signals, and cell fate. Curr Opin Immunol. 2017; 46:viii–xi. [PubMed: 28684058]
26. MacIver NJ, Michalek RD, Rathmell JC. Metabolic regulation of T lymphocytes. Annu Rev Immunol. 2013; 31:259–83. [PubMed: 23298210]
27. Coloff JL, Macintyre AN, Nichols AG, Liu T, Gallo CA, Plas DR, Rathmell JC. Akt-dependent glucose metabolism promotes Mcl-1 synthesis to maintain cell survival and resistance to Bcl-2 inhibition. Cancer Res. 2011; 71:5204–13. [PubMed: 21670080]

28. Patsoukis N, Bardhan K, Chatterjee P, Sari D, Liu B, Bell LN, Karoly ED, Freeman GJ, Petkova V, Seth P, Li L, Boussiotis VA. PD-1 alters T-cell metabolic reprogramming by inhibiting glycolysis and promoting lipolysis and fatty acid oxidation. Nat Commun. 2015; 6:6692. [PubMed: 25809635]
29. He W, Zhang H, Han F, Chen X, Lin R, Wang W, Qiu H, Zhuang Z, Liao Q, Zhang W, Cai Q, Cui Y, Jiang W, Wang H, Ke Z. CD155T/TIGIT Signaling Regulates CD8(+) T-cell Metabolism and Promotes Tumor Progression in Human Gastric Cancer. Cancer Res. 2017; 77:6375–88. [PubMed: 28883004]
30. Hogquist KA, Jameson SC, Heath WR, Howard JL, Bevan MJ, Carbone FR. T cell receptor antagonist peptides induce positive selection. Cell. 1994; 76:17–27. [PubMed: 8287475]
31. Barnden MJ, Allison J, Heath WR, Carbone FR. Defective TCR expression in transgenic mice constructed using cDNA-based alpha- and beta-chain genes under the control of heterologous regulatory elements. Immunol Cell Biol. 1998; 76:34–40. [PubMed: 9553774]
32. Ehst BD, Ingulli E, Jenkins MK. Development of a novel transgenic mouse for the study of interactions between CD4 and CD8 T cells during graft rejection. Am J Transplant. 2003; 3:1355–62. [PubMed: 14525595]
33. Trambley J, Bingaman AW, Lin A, Elwood ET, Waitze SY, Ha J, Durham MM, Corbascio M, Cowan SR, Pearson TC, Larsen CP. Asialo GM1(+) CD8(+) T cells play a critical role in costimulation blockade-resistant allograft rejection. J Clin Invest. 1999; 104:1715–22. [PubMed: 10606625]
34. Liu D, Krummey SM, Badell IR, Wagener M, Schneeweis LA, Stetsko DK, Suchard SJ, Nadler SG, Ford ML. 2B4 (CD244) induced by selective CD28 blockade functionally regulates allograft-specific CD8+ T cell responses. J Exp Med. 2014; 211:297–311. [PubMed: 24493803]
35. Lee C-F, Lo Y-C, Cheng C-H, Furtmüller GJ, Oh B, Andrade-Oliveira V, Thomas AG, Bowman CE, Slusher BS, Wolfgang MJ, Brandacher G, Powell JD. Preventing allograft rejection by targeting immune metabolism. Cell reports. 2015; 13:760–70. [PubMed: 26489460]
36. Patsoukis N, Bardhan K, Chatterjee P, Sari D, Liu B, Bell LN, Karoly ED, Freeman GJ, Petkova V, Seth P, Li L, Boussiotis VA. PD-1 alters T-cell metabolic reprogramming by inhibiting glycolysis and promoting lipolysis and fatty acid oxidation. Nature Communications. 2015; 6:6692.
37. Frauwirth KA, Thompson CB. Regulation of T Lymphocyte Metabolism. The Journal of Immunology. 2004; 172:4661–5. [PubMed: 15067038]
38. Phan Anthony T, Doedens Andrew L, Palazon A, Tyrakis Petros A, Cheung Kitty P, Johnson Randall S, Goldrath Ananda W. Constitutive Glycolytic Metabolism Supports $CD8^{+}$ T Cell Effector Memory Differentiation during Viral Infection. Immunity. 45:1024–37.
39. Le A, Lane AN, Hamaker M, Bose S, Gouw A, Barbi J, Tsukamoto T, Rojas CJ, Slusher BS, Zhang H, Zimmerman LJ, Liebler DC, Slebos RJ, Lorkiewicz PK, Higashi RM, Fan TW, Dang CV. Glucose-independent glutamine metabolism via TCA cycling for proliferation and survival in B cells. Cell Metab. 2012; 15:110–21. [PubMed: 22225880]
40. Wherry EJ, Ha SJ, Kaech SM, Haining WN, Sarkar S, Kalia V, Subramaniam S, Blattman JN, Barber DL, Ahmed R. Molecular Signature of CD8(+) T Cell Exhaustion during Chronic Viral Infection. Immunity. 2007
41. Floyd TL, Koehn BH, Kitchens WH, Robertson JM, Cheeseman JA, Stempora L, Larsen CP, Ford ML. Limiting the amount and duration of antigen exposure during priming increases memory T cell requirement for costimulation during recall. J Immunol. 2011; 186:2033–41. [PubMed: 21257960]
42. Liu D, Badell IR, Ford ML. Selective CD28 blockade attenuates CTLA-4-dependent CD8+ memory T cell effector function and prolongs graft survival. JCI Insight. 2018; 3
43. Moro-García MA, Mayo JC, Sainz RM, Alonso-Arias R. Influence of Inflammation in the Process of T Lymphocyte Differentiation: Proliferative, Metabolic, and Oxidative Changes. Frontiers in Immunology. 2018; 9
44. Bengsch B, Johnson AL, Kurachi M, Odorizzi PM, Pauken KE, Attanasio J, Stelekati E, McLane LM, Paley MA, Delgoffe GM, Wherry EJ. Bioenergetic Insufficiencies Due to Metabolic Alterations Regulated by the Inhibitory Receptor PD-1 Are an Early Driver of CD8(+) T Cell Exhaustion. Immunity. 2016; 45:358–73. [PubMed: 27496729]

45. Chatterjee P, Sari D, Petkova V, Li L, Boussiotis VA. PD-1 Induces Metabolic Reprogramming Of Activated T Cells From Glycolysis To Lipid Oxidation. Blood. 2013; 122:187.

46. Wahl DR, Byersdorfer CA, Ferrara JLM, Opipari AW, Glick GD. Distinct metabolic programs in activated T cells: opportunities for selective immunomodulation. Immunological Reviews. 2012; 249:104–15. [PubMed: 22889218]

47. Sukumar M, Liu J, Ji Y, Subramanian M, Crompton JG, Yu Z, Roychoudhuri R, Palmer DC, Muranski P, Karoly ED, Mohney RP, Klebanoff CA, Lal A, Finkel T, Restifo NP, Gattinoni L. Inhibiting glycolytic metabolism enhances CD8+ T cell memory and antitumor function. J Clin Invest. 2013; 123:4479–88. [PubMed: 24091329]

48. van der Windt GJ, O'Sullivan D, Everts B, Huang SC, Buck MD, Curtis JD, Chang CH, Smith AM, Ai T, Faubert B, Jones RG, Pearce EJ, Pearce EL. CD8 memory T cells have a bioenergetic advantage that underlies their rapid recall ability. Proc Natl Acad Sci U S A. 2013; 110:14336–41. [PubMed: 23940348]

49. Chang CH, Curtis JD, Maggi LB Jr, Faubert B, Villarino AV, O'Sullivan D, Huang SC, van der Windt GJ, Blagih J, Qiu J, Weber JD, Pearce EJ, Jones RG, Pearce EL. Posttranscriptional control of T cell effector function by aerobic glycolysis. Cell. 2013; 153:1239–51. [PubMed: 23746840]

50. Krummey SM, Floyd TL, Liu D, Wagener ME, Song M, Ford ML. Candida-elicited murine Th17 cells express high Ctla-4 compared with Th1 cells and are resistant to costimulation blockade. J Immunol. 2014; 192:2495–504. [PubMed: 24493820]

51. Vincenti F, Rostaing L, Grinyo J, Rice K, Steinberg S, Gaite L, Moal MC, Mondragon-Ramirez GA, Kothari J, Polinsky MS, Meier-Kriesche HU, Munier S, Larsen CP. Belatacept and Long-Term Outcomes in Kidney Transplantation. N Engl J Med. 2016; 374:333–43. [PubMed: 26816011]

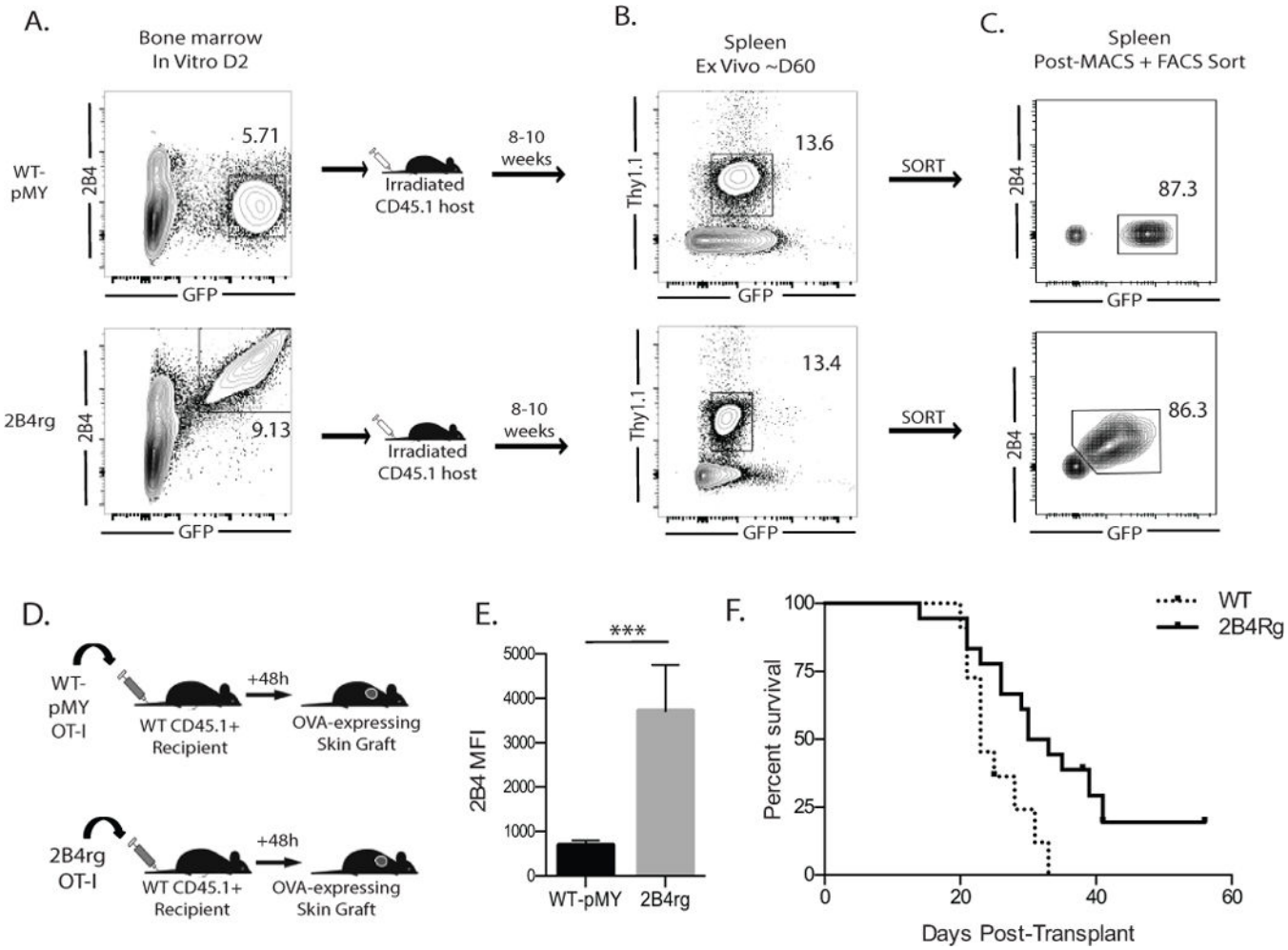

Figure 1. Generation of retrogenic graft-specific CD8$^+$ T cells that constitutively express 2B4

A, Frequencies of GFP$^+$ (pMY control vector) or GFP$^+$ 2B4$^+$ (for 2B4 vector) CD45.2$^+$ Thy1.1$^+$ OT-I BM cells at d2. B, BM cells were adoptively transferred into irradiated CD45.1$^+$ Thy1.2$^+$ animals and were detectable at 8–10 weeks. C, GFP$^+$ CD8$^+$ Thy1.1$^+$ (pMY) and GFP$^+$ 2B4$^+$ CD3$^+$ Thy1.1$^+$ (2B4rg) OT-I T cells sorted and D, adoptively transferred (10^6/recipient) into naïve B6 hosts that received two OVA-expressing skin grafts 48 hours later. Data shown in A–D are representative of 11-12 mice/group from 3 independent experiments.

E, 2B4 expression is maintained on the retrovirally transduced retrogenic cells following transplantation. F, 10^6 WT CD8$^+$ Thy1.1$^+$ or GFP$^+$ 2B4$^+$ CD3$^+$ Thy1.1$^+$ (2B4rg) OT-I T cells were adoptively transferred naïve B6 hosts 48 hours prior to receiving two OVA-expressing skin grafts. Animals received 250 μg of CTLA4Ig on post-operative Day 0, 2, 4, and 6. Graft survival was measured, and rejection was scored based on a loss of +90% viable tissue. Data shown in Figure 1 A–E are representative of 11-12 mice/group from 3 independent experiments. $^{***}p<0.0001$. Data shown in Figure 1F are representative of 12-18 mice/group from 2 independent experiments.

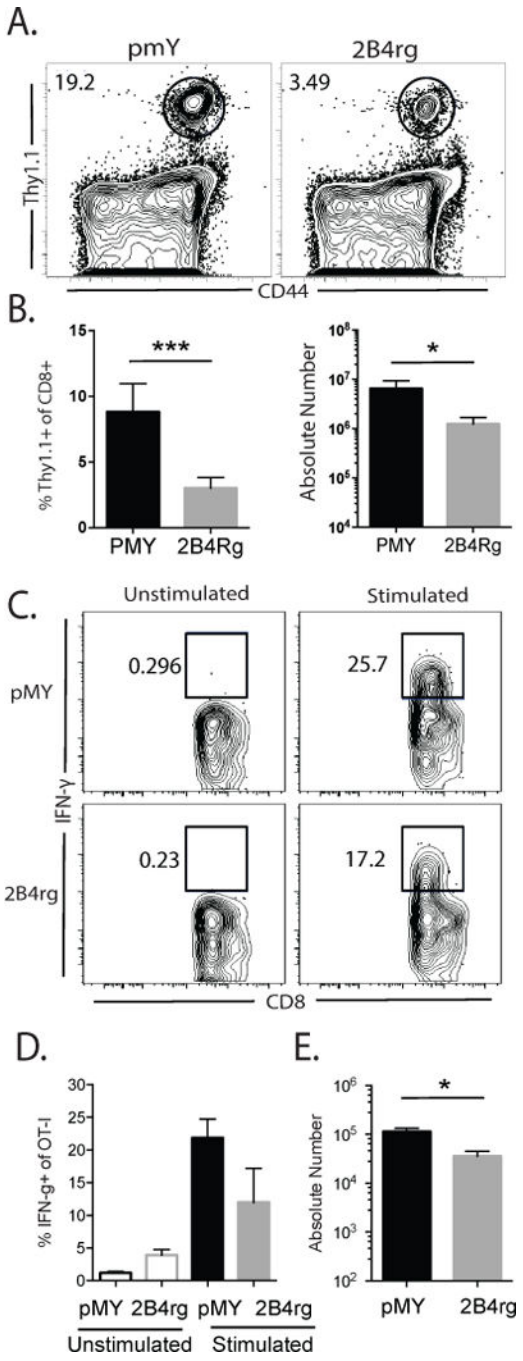

Figure 2. Ectopic expression of 2B4 results in reduced accumulation of antigen-specific CD8$^+$ T cells but does not impact function of antigen-specific CD8$^+$ T cells on a per cell basis

A, Representative flow cytometry plots gated on CD8$^+$ cells isolated from the spleen. B, Frequencies and absolute numbers of CD44^{hi} Thy1.1$^+$ of CD8$^+$ cells. C, IFN-γ$^+$ pMY or 2B4rg cells following *ex vivo* stimulation with PMA and ionomycin. D, Summary of the frequency of IFN-γ-producing Thy1.1$^+$ CD8$^+$ T cells, representative of 2 independent experiments with 7-8 mice/group. E, Summary of the absolute numbers of IFN-γ-producing Thy1.1$^+$ CD8$^+$ T cells, representative of 2-3 independent experiments with 7-12 mice/group. $^*p<0.05$, $^{**}p<0.001$, $^{***}p<0.0001$.

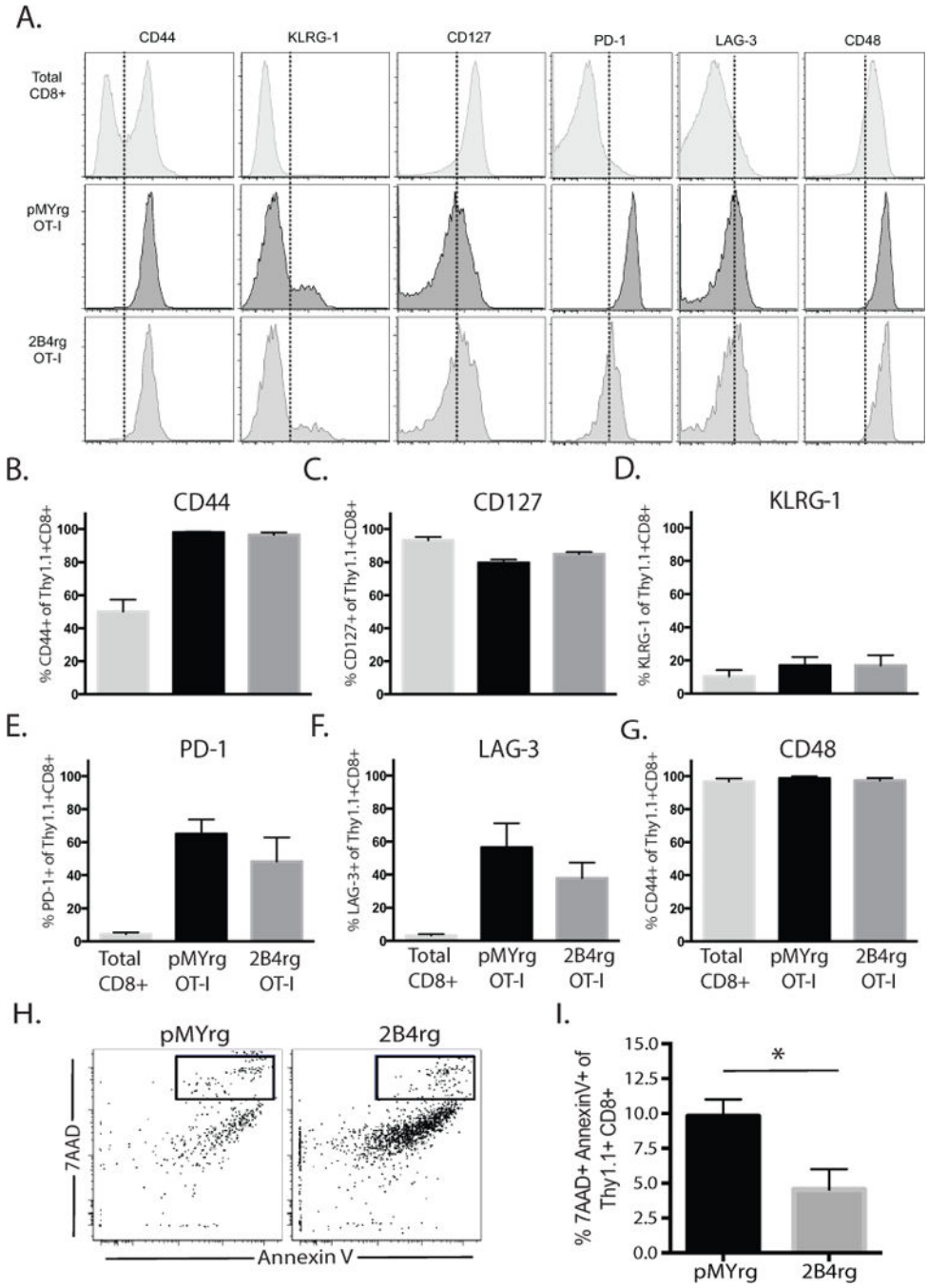

Figure 3. Failure of 2B4 retrogenic cells to accumulate in the spleen is not due to differences in expression of the 2B4 ligand or of T cell activation or exhaustion markers

Naïve B6 animals received 10^6 2B4rg Thy1.1$^+$ OT-I T cells or pMY Thy1.1$^+$ OT-I controls and were challenged with OVA-expressing skin grafts. A, Representative flow histograms indicating expression intensity of CD44, CD48, CD127, KLRG-1, PD-1, and LAG-3 on CD8$^+$ Thy1.1$^+$ T cells isolated from the spleen 10 days following transplantation. B-G, Summary of the frequencies of CD44^{hi}, CD48$^+$, CD127$^+$, KLRG-1$^+$, PD-1$^+$, and LAG-3$^+$ CD8$^+$ Thy1.1$^+$ T cells isolated from the spleen on day 10. H-I, Representative flow dot plots

and summary bar graphs illustrating the frequency of Annexin V and 7AAD double-positive OT-I T cells 10 days after transplantation.

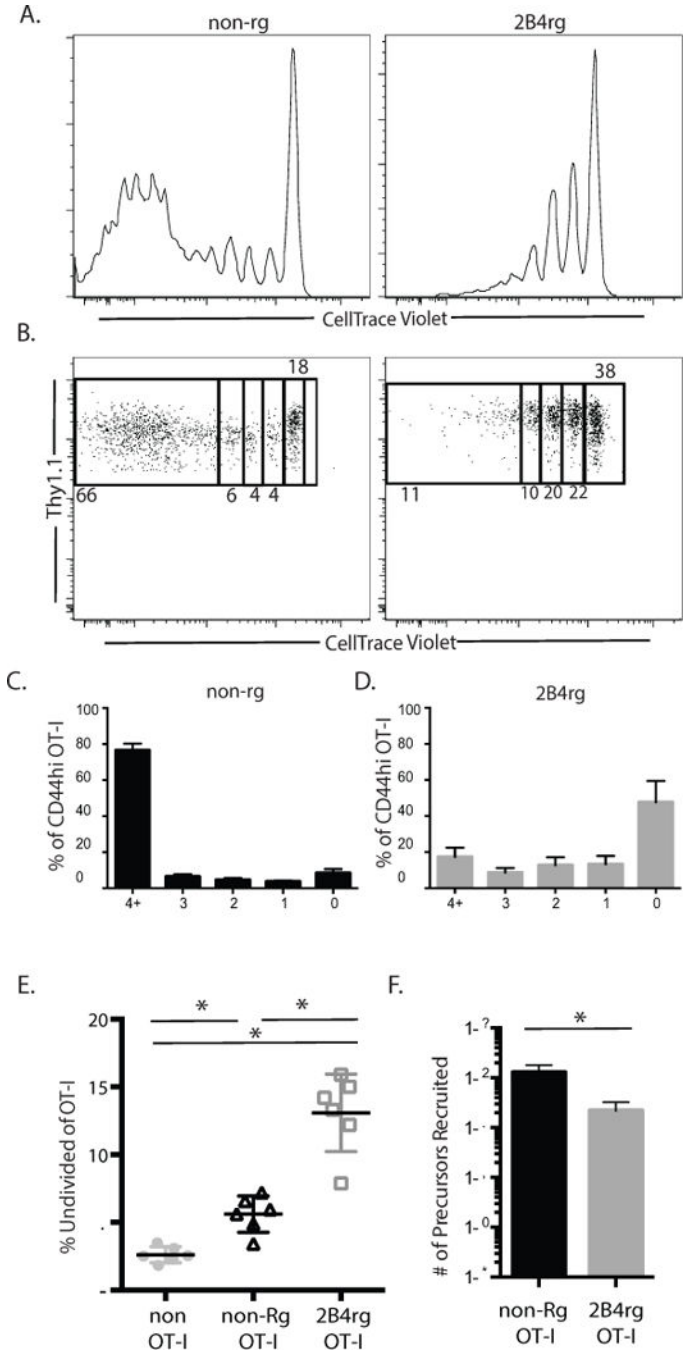

Figure 4. 2B4 rg cells undergo less division compared to their empty-vector pMY control counterparts

A and B, CTV dilution of Thy1.1$^+$ CD8$^+$ 2B4rg and Thy1.1$^+$ CD8$^+$ non-rg OT-I controls on day 10. C-D, Summary of frequency of 2B4rg and control OT-I T cells in each round of division. E, Frequencies of undivided CD8$^+$ T cells in the spleen on d 10. F, Summary of the number of Thy1.1$^-$ CD8$^+$ non-OT-I and Thy1.1$^+$ CD8$^+$ OT-I T precursors recruited into the anti-donor immune response. All data are representative of two independent experiments with a total of 9-11 mice/group. $p < 0.05$.

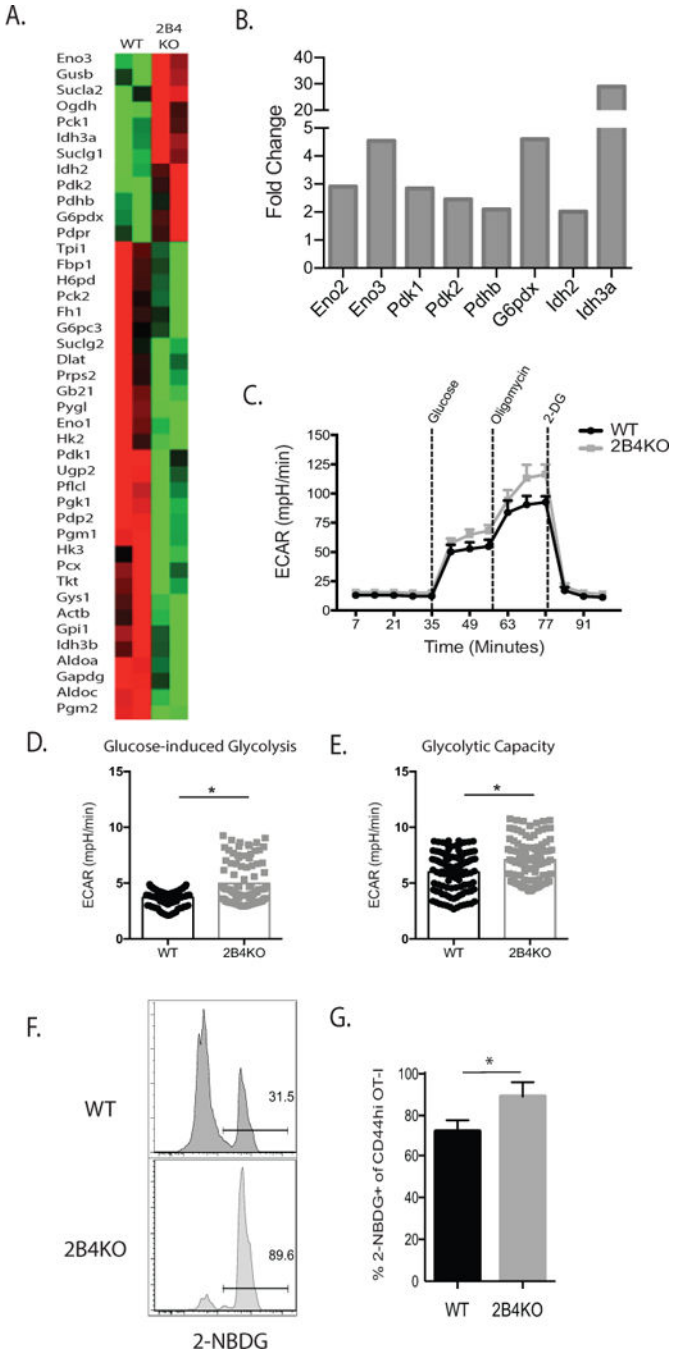

Figure 5. 2B4 signaling limits glycolytic capacity of CD8$^+$ T cells

A, cDNA was synthesized from 400 ng of RNA isolated from 2B4$^+$ WT or 2B4KO OT-I T cells following *in vitro* activation (7d) and restimulation (4d) and subsequently used to assess changes in glycolytic metabolism between 2B4$^+$ and 2B4KO cells via the Qiagen Glucose Metabolism RT^2 Profiler PCR Array. Representative of 2 independent experiments with a total of 6-8 mice per group. B, Summary derived from the data set described above in A of selected genes that were increased over baseline in OT-I T cells in the absence of 2B4. C, 3×10^6 WT or 2B4KO OT-I T cells were stimulated with 1nM SIINFEKL for 4 d. 2×10^5

OT-I Ficoll-purified cells were then plated as described in Supplemental Methods. D-E, Rate of ECAR during glucose-induced glycolysis was averaged from three measurements following the addition of glucose, while glycolytic capacity was calculated from the average of three measurements following the addition of oligomycin. C-E are representative of two experiments, $p < 0.0001$. F, 10^4 WT or 2B4KO OT-I T cells were transferred into naïve B6 hosts and infected with 10^4 CFU of LM-OVA two days later. After 14 days, recipients were sacrificed, splenocytes were prepared as a single-cell suspension, washed with PBS, and then incubated with 2-NBDG *ex vivo* and analyzed via flow cytometry. G, Summary of expression of 2-NBDG as gated in part F. $p = 0.01$. F-G are representative of 4-5 mice/group.

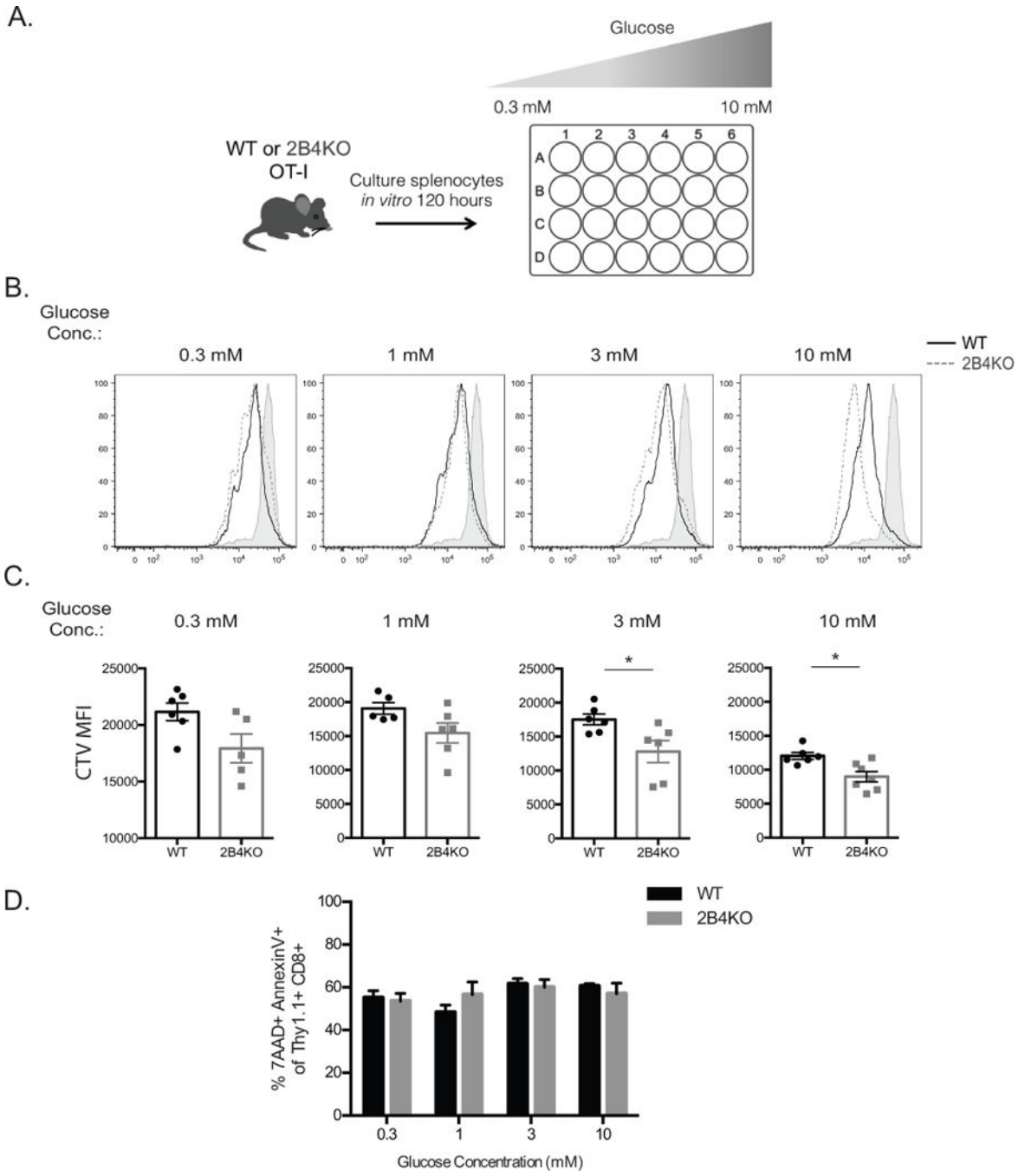

Figure 6. Proliferative advantage of 2B4 KO T cells is erased under glucose limiting conditions

A, 3×10^6 WT and 2B4KO OT-I T cells, respectively, were resuspended in complete media and a D-glucose solution was titered into the glucose-free complete media and diluted on a half-log scale. Cells were then stimulated with SIINFEKL N4 peptide at 1 nM for 5 days. After 5 days in culture cells were harvested and stained for flow cytometry and CTV-dilution of Thy1.1$^+$ CD8$^+$ antigen-reactive T cells was assessed. B-C, Representative flow cytograms and summary data depicting dilution of CTV in Thy1.1$^+$ OT-I T cell compartments under glucose-limiting culture conditions. D, Summary data depicting frequency of 7AAD and

AnnexinV double positive apoptotic cells from each culture condition. Data are representative of 2 independent experiments with a total of 6-8 animals per group. p = 0.01

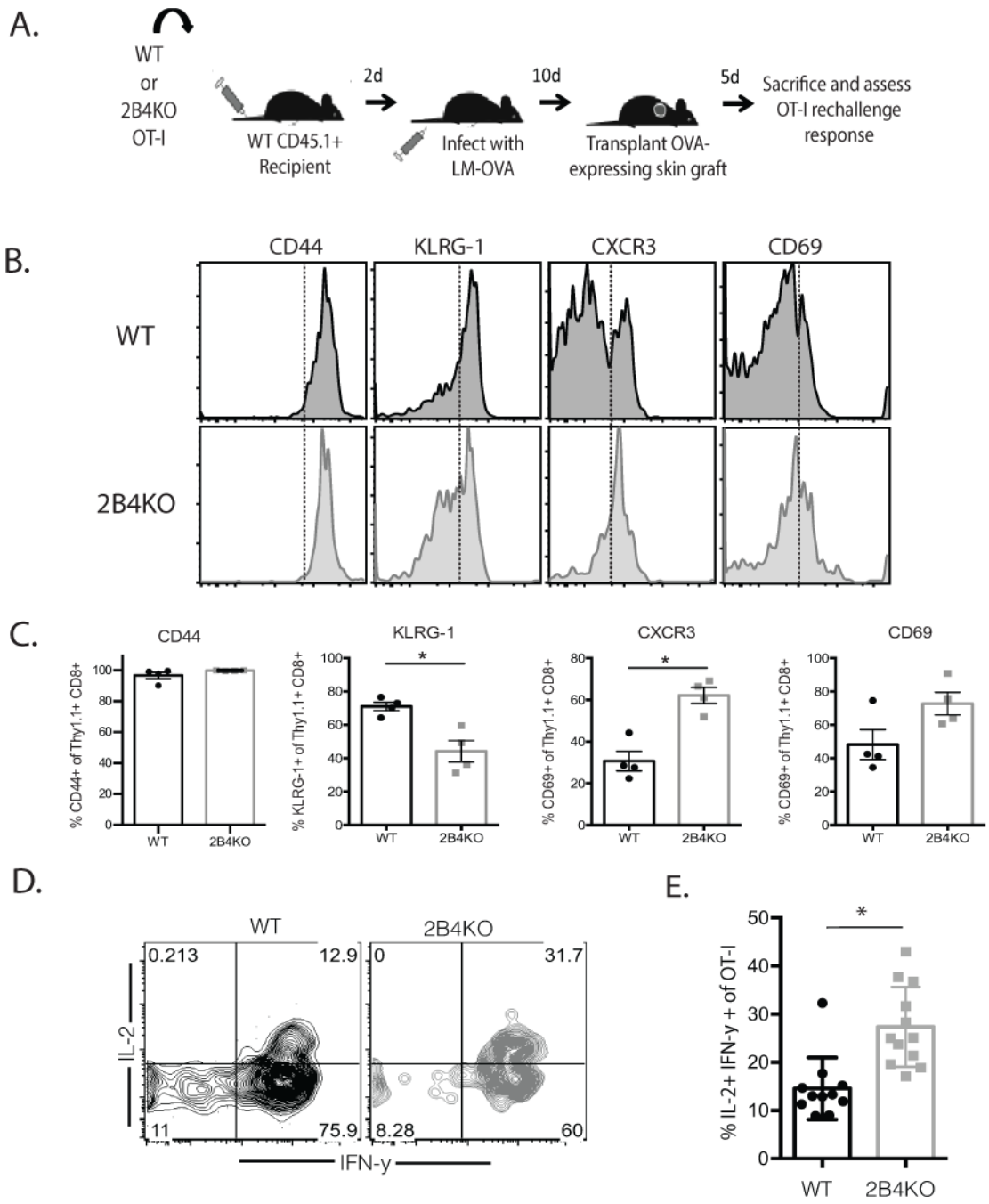

Figure 7. 2B4-mediated signals impact memory recall potential

A, 10^4 WT or 2B4KO OT-I T cells were transferred into naïve B6 hosts, which were infected with 10^4 CFU LM-OVA 2d later. Animals received OVA-expressing skin grafts at day 10 post-transplant and were sacrificed five days later. B-C, Representative flow cytograms and summary data depicting the expression of CD44, KLRG-1, CXCR3, and CD69 on Thy1.1$^+$ CD8$^+$ OT-I T cells isolated from the spleen. D-E, Splenocytes were restimulated *ex vivo* with PMA and ionomycin and analyzed by ICS. Data shown in A–E are representative of 6-11 mice/group from 2 independent experiments. p = 0.0005.